Chapter 4

Phyllotaxis

The regular arrangement of lateral organs (leaves on a stem, scales on a cone axis, florets in a composite flower head) is an important aspect of plant form, known as *phyllotaxis*. The extensive literature generated by biologists' and mathematicians' interest in phyllotaxis is reviewed by Erickson [36] and Jean [78]. The proposed models range widely from purely geometric descriptions (for example, Coxeter [17]) to complex physiological hypotheses tested by computer simulations (Hellendoorn and Lindenmayer [59], Veen and Lindenmayer [151], Young [163]). This chapter presents two models suitable for the synthesis of realistic images of flowers and fruits that exhibit spiral phyllotactic patterns.

Both models relate phyllotaxis to packing problems. The first operates in a plane and was originally proposed by Vogel [154] to describe the structure of a sunflower head. A further detailed analysis was given by Ridley [124, 125]. The second model reduces phyllotaxis to the problem of packing circles on the surface of a cylinder. Its analysis was presented by van Iterson [75] and reviewed extensively by Erickson [36].

The area of phyllotaxis is dominated by intriguing mathematical relationships. One of them is the "remarkable fact that the numbers of spirals which can be traced through a phyllotactic pattern are predominantly integers of the Fibonacci sequence" [36, p. 54]. For example, Coxeter [17] notes that the pineapple displays eight rows of scales sloping to the left and thirteen rows sloping to the right. Furthermore, it is known that the ratios of consecutive Fibonacci numbers F_{k+1}/F_k converge towards the golden mean $\tau = (\sqrt{5}+1)/2$. The *Fibonacci angle* $360°\tau^{-2}$, approximately equal to 137.5°, is the key to the first model discussed in this chapter.

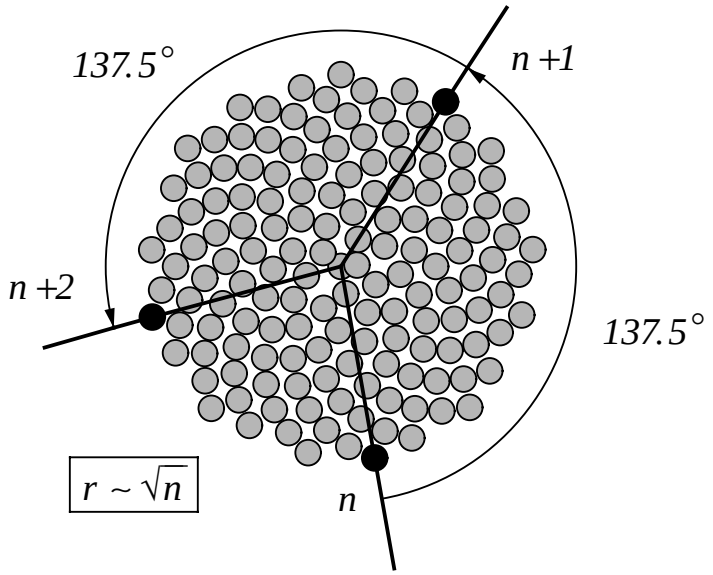


```
#define a 137.5  /* divergence angle */
#include D       /* disk shape specification */

ω  :  A(0)
p1 :  A(n) :  * → +(a)[f(n^0.5)~D]A(n+1)
```

Figure 4.1: Pattern of florets in a sunflower head, according to Vogel's formula

4.1 The planar model

Vogel's formula

In order to describe the pattern of florets (or seeds) in a sunflower head, Vogel [154] proposed the formula

$$\phi = n * 137.5^\circ, \qquad r = c\sqrt{n}, \tag{4.1}$$

where:

- n is the ordering number of a floret, counting outward from the center. This is the reverse of floret age in a real plant.
- ϕ is the angle between a reference direction and the position vector of the n^{th} floret in a polar coordinate system originating at the center of the capitulum. It follows that the *divergence angle* between the position vectors of any two successive florets is constant, $\alpha = 137.5^\circ$.
- r is the distance between the center of the capitulum and the center of the n^{th} floret, given a constant scaling parameter c.

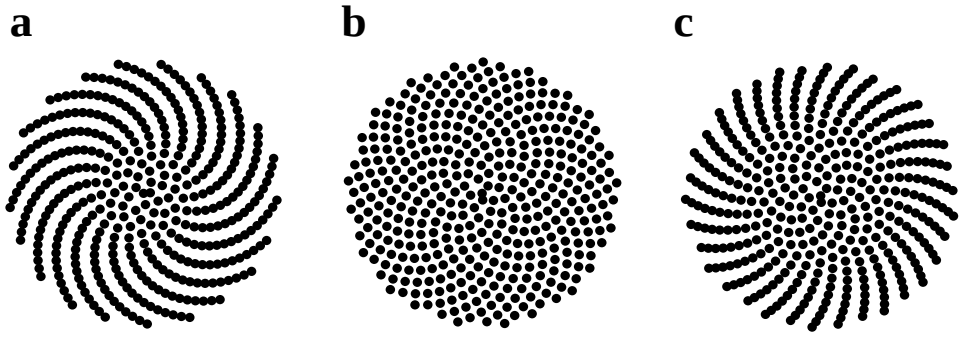

Figure 4.2: Generating phyllotactic patterns on a disk. These three patterns differ only by the value of the divergence angle α, equal to (a) 137.3°, (b) 137.5° (the correct value), and (c) 137.6°.

Model justification

The distribution of florets described by formula (4.1) is shown in Figure 4.1. The square-root relationship between the distance r and the floret ordering number n has a simple geometric explanation. Assuming that all florets have the same size and are densely packed, the total number of florets that fit inside a disc of radius r is proportional to the disk area. Thus, the ordering number n of the most outwardly positioned floret in the capitulum is proportional to r^2, or $r \sim \sqrt{n}$.

The divergence angle of 137.5° is much more difficult to explain. Vogel [154] derives it using two assumptions.

- Each new floret is issued at a fixed angle α with respect to the preceding floret.
- The position vector of each new floret fits into the largest existing gap between the position vectors of the older florets.

Ridley [125] does not object to these basic assumptions, but indicates that they are insufficient to explain the origin of the Fibonacci angle, and points to several arbitrary steps present in Vogel's derivation. He describes the main weakness as follows:

> While it is reasonable to assume that the plant could contain genetic information determining the divergence angle to some extent, it is completely impossible for this alone to fix the divergence angle to the incredible accuracy occurring in nature, since natural variation in biological phenomena is normally rather wide. For example, for the 55- and 89-parastichies to be conspicuous, as occurs in most sunflower heads, d must lie between $\frac{21}{55}$ and $\frac{34}{89}$, a relative accuracy of one part in 1869.

The critical role of the divergence angle α is illustrated in Figure 4.2.

Figure 4.3: Close-up of a daisy capitulum

Parastichies

Although a comprehensive justification of Vogel's formula may require further research, the model correctly describes the arrangement of florets visible in actual capitula. The most prominent feature is two sets of spirals or *parastichies*, one turning clockwise, the other counterclockwise, which are composed of nearest neighboring florets. The number of spirals in each set is always a member of the Fibonacci sequence; 21 and 34 for a small capitulum, up to 89 and 144 or even 144 and 233 for large ones. For example, the capitulum of a daisy (Figure 4.3) exhibits 34 clockwise spirals and 21 counterclockwise spirals, with directions determined by following the spirals outwards from the capitulum center. In the image of a domestic sunflower capitulum (Figure 4.4), one can discern 34 spirals running clockwise and 55 spirals running counterclockwise. The number of perceived spirals depends on the capitulum size expressed in terms of the number of component florets. If the field of attention is limited to a circle approximately 2/3 the size of the entire sunflower capitulum in Figure 4.4, the number of discernible spirals becomes 34 and 21.

Figure 4.4: Domestic sunflower head →

```
#define S         /* seed shape */
#define R         /* ray floret shape */
#include M N O P  /* petal shapes */

ω  :  A(0)
p1 :  A(n) :  * → +(137.5)[f(n^0.5)C(n)]A(n+1)
p2 :  C(n) :  n <= 440            → ~S
p3 :  C(n) :  440 < n & n <= 565  → ~R
p4 :  C(n) :  565 < n & n <= 580  → ~M
p5 :  C(n) :  580 < n & n <= 595  → ~N
p6 :  C(n) :  595 < n & n <= 610  → ~O
p7 :  C(n) :  610 < n             → ~P
```

The dependence of the number of parastichies on the size of the field of attention is yet another intriguing aspect of spiral phyllotaxis, as pointed out in the following excerpt from a letter by Alan Turing [1] quoted in [18]:

> According to the theory I am working on now there is a continuous advance from one pair of parastichy numbers to another, during the growth of a single plant. ... You will be inclined to ask how one can move continuously from one integer to another. The reason is this — on any specimen there are different ways in which the parastichy numbers can be reckoned; some are more natural than others. During the growth of a plant the various parastichy numbers come into prominence at different stages. One can also observe the phenomenon in space (instead of in time) on a sunflower. It is natural to count the outermost florets as say $21 + 34$, but the inner ones might be counted as $8 + 13$. ... I don't know any really satisfactory account, though I hope to get one myself in about a year's time.

Sunflower head

A complete model of a flower head, suitable for realistic image synthesis, should contain several organs of various shapes. This is easily achieved by associating different surfaces with specific ranges of the index n. For example, consider the L-system that generates the sunflower head (Figure 4.4). The layout of components is specified by production p_1, similar to that of the L-system in Figure 4.1. Productions p_2 to p_7 determine colors and shapes of components as a function of the derivation step number. The entire structure shown in Figure 4.4 was generated in 630 steps. Alternatively, random selection of similar surfaces could have been employed to prevent the excessive regularity of the resulting image.

Other extensions to the basic model consist of varying organ orientation in space and changing their altitude from the plane of the head as a function of n. For example, the sunflower plants included in Figure 4.5 have flowers in four developmental stages: buds, young flowers starting to open, open flowers and older flowers where the petals begin to droop. All flowers are generated using approximately the same number of florets. The central florets are represented by the same surface at each stage. The shape and orientation of surfaces representing petals vary from one stage to another. The plants have been modeled as dibotryoids, with a single signal inducing a basipetal flowering sequence, as described in the previous chapter.

[1] To computer scientists, Alan Turing is best known as the inventor of the *Turing machine* [146], which plays an essential role in defining the notion of an algorithm. However, biologists associate Turing's name primarily with his 1952 paper, "The chemical basis of morphogenesis" [147], which pioneered the use of mathematical models in the study of pattern formation and advocated the application of computers to simulate biological phenomena.

Figure 4.5: Sunflower field

Figure 4.6: Zinnias

Other examples

The zinnias (Figures 4.6 and 4.7) illustrate the effect of changing a petal's altitude, size and orientation as a function of n. The height at which a petal is placed decreases by a small amount as n increases. The size of each successive petal is incremented linearly. The orientation is also adjusted linearly by a small angle increment. Thus, petals with small values of index n are placed more vertically, while petals with larger indices n are more horizontal. Although the family Compositae offers the most examples of phyllotactic patterns, the same model can be applied to synthesize images of other flowers, such as water-lilies (Figures 4.8 and 4.9) and roses (Figure 4.10).

Figure 4.7: Close-up of zinnias →

Figure 4.8: Water-lily

Figure 4.9: Lily pond

Figure 4.10: Roses

4.2 The cylindrical model

Basic model

The spiral patterns evident in elongated organs such as pine cones, fir cones and pineapples, can be described by models that position components, in this case scales, on the surface of a cylinder. Van Iterson [75] divides phyllotactic patterns on cylinders into *simple* and *conjugate* ones. In the case of a simple arrangement, all components lie on a single *generative helix*. In contrast, conjugate patterns consist of two or more interleaved helices. This paper discusses simple phyllotactic patterns only. They are generally characterized by the formula

$$\phi = n * \alpha, \qquad r = const, \qquad H = h * n, \tag{4.2}$$

where:

- n is the ordering number of a scale, counting from the bottom of the cylinder;
- ϕ, r and H are the cylindrical coordinates of the n^{th} scale;
- α is the divergence angle between two consecutive scales (as in the planar case, it is assumed to be constant); and
- h is the vertical distance between two consecutive scales (measured along the main axis of the cylinder).

Implementation using L-systems

A parametric L-system that generates the pattern described by formula (4.2) is given in Figure 4.11. The operation of this L-system simulates the natural process of subapical development characterized by sequential production of consecutive modules by the top part of the growing plant or organ. The apex A produces internodes $f(h)$ along the main axis of the modeled structure. Associated with each internode is a disk $\sim D$ placed at a distance r from the axis. This offset is achieved by moving the disk away from the axis using the module $f(r)$, positioned at a right angle with respect to the axis by $\&(90)$. The spiral disk distribution is due to the module $/(a)$, which rotates the apex around its own axis by the divergence angle in each derivation step.

Analysis of model geometry

In the planar model, the constant divergence angle $\alpha = 137.5°$ is found across a large variety of flower heads. The number of perceived parastichies is determined by the capitulum size, and it changes as the distance from the capitulum center increases. In contrast, a phyllotactic pattern on the surface of a cylinder is uniform along the entire cylinder length. The number of evident parastichies depends on the values of parameters α and h. The key problem, both from the viewpoint of understanding the geometry of the pattern and applying it to generate synthetic images, is to express the divergence angle α and the vertical displacement h as a function of the numbers of evident parastichies encircling the cylinder in the clockwise and counterclockwise directions. A solution to this problem was proposed by van Iterson [75] and reviewed by Erickson [36]. Our presentation closely follows that of Erickson.

The phyllotactic pattern can be explained in terms of circles packed on the surface of the cylinder. An evident parastichy consists of a sequence of tangent circles, the ordering numbers of which form an arithmetic sequence with difference m. The number m is referred to as the *parastichy order*. Thus, the circles on the cylinder surface may be arranged in two congruent 2-parastichies, five congruent 5-parastichies, and so on. The angular displacement between two consecutive circles in an m-parastichy is denoted by δ_m. By definition, δ_m belongs to the range $(-\pi, \pi]$ radians. The relation between the angular displacement δ_m and the divergence angle α is expressed by the equation

$$\delta_m = m\alpha - \Delta_m 2\pi, \tag{4.3}$$

where Δ_m is an integer called the *encyclic number*. It is the number of turns around the cylinder, rounded to the nearest integer, which the generative helix describes between two consecutive points of the m-parastichy.

Usually, one can perceive two series of parastichies running in opposite directions (Figure 4.11). The second parastichy satisfies an equation analogous to (4.3):

$$\delta_n = n\alpha - \Delta_n 2\pi \tag{4.4}$$

Consider the m- and n-parastichies starting at circle 0. In their paths across the cylinder, they will intersect again at circle mn. Assume

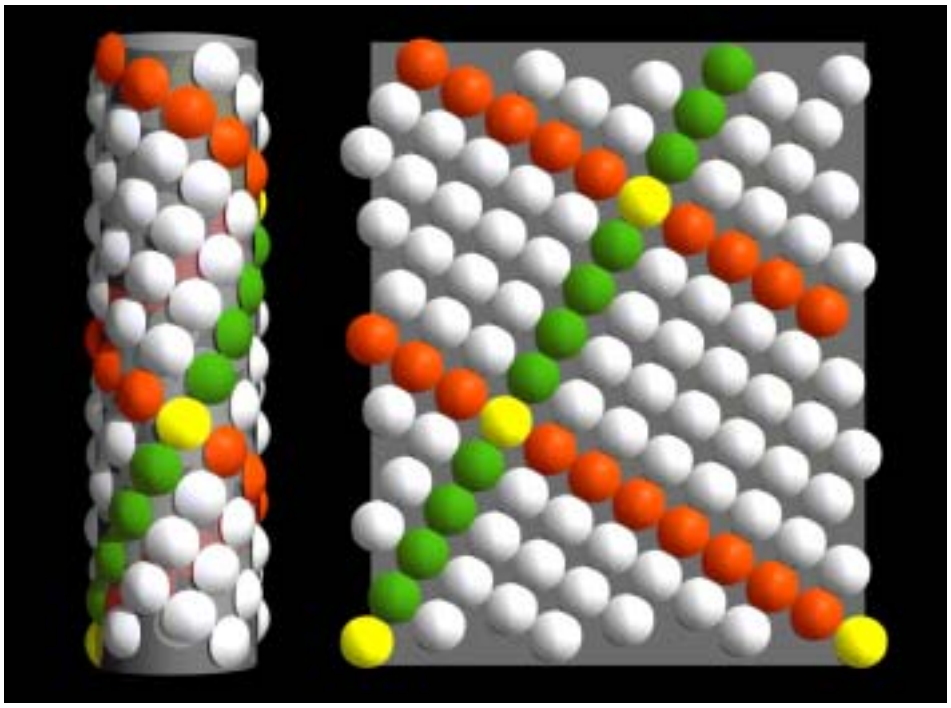

```
#define a 137.5281  /* divergence angle */
#define h 35.3      /* vertical displacement */
#define r 500       /* component offset from main axis */
#include D          /* disk shape specification */

ω  :  A
p1 :  A : * → [&(90)f(r)∼D]f(h)/(a)A
```

Figure 4.11: Parastichies on the surface of a cylinder and on the unrolled cylinder. The L-system generates the cylindrical pattern.

that m and n are relatively prime; otherwise the phyllotactic pattern would have to contain several circles lying at the same height H and, contrary to the initial assumption, would not be simple. The circle mn is the first point of intersection between the m-parastichy and the n-parastichy above circle 0. Consequently, the path from circle 0 to mn along the m-parastichy, and back to 0 along the n-parastichy, encircles the cylinder exactly once. The section of m-parastichy between circles 0 and mn consists of $n+1$ circles (including the endpoints), so the angular distance between the circles 0 and mn is equal to $n\delta_m$. Similarly, the distance between circles 0 and mn, measured along the n-parastichy, can be expressed as $m\delta_n$. As a result,

$$n\delta_m - m\delta_n = \pm 2\pi. \tag{4.5}$$

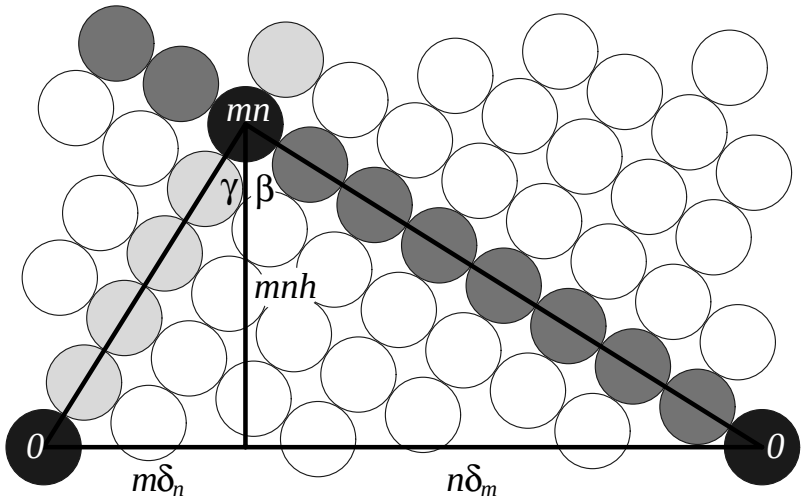

Figure 4.12: An opposite parastichy triangle (as in Erickson [36, Fig. 3.8]). The base is formed by the circumference of the cylinder. The sides are formed by the parastichies.

The signs in equation (4.5) correspond to the assumption that the spirals encircle the cylinder in opposite directions; thus one of the values δ is positive and the other one is negative. Substituting the right sides of equations (4.3) and (4.4) for δ_m and δ_n yields

$$n\Delta_m - m\Delta_n = \pm 1. \tag{4.6}$$

To further analyze the pertinent geometric relationships, the cylinder is cut along the vertical line passing through the center of circle 0 and "unrolled" (Figure 4.11). The two parastichies and the circumference of the cylinder passing through point 0 form a triangle as shown in Figure 4.12. The perpendicular to the base from point mn divides this triangle into two right triangles. If d denotes the diameter of the circles, then

$$(n\delta_m)^2 + (mnh)^2 = (nd)^2$$

and

$$(m\delta_n)^2 + (mnh)^2 = (md)^2.$$

The above system of equations can be solved with respect to h and d:

$$h = \sqrt{(\delta_m^2 - \delta_n^2)/(n^2 - m^2)} \tag{4.7}$$

$$d = \sqrt{(n^2\delta_m^2 - m^2\delta_n^2)/(n^2 - m^2)} \tag{4.8}$$

or, taking into consideration equation (4.5),

$$d = \sqrt{2\pi(n\delta_m + m\delta_n)/(n^2 - m^2)}. \tag{4.9}$$

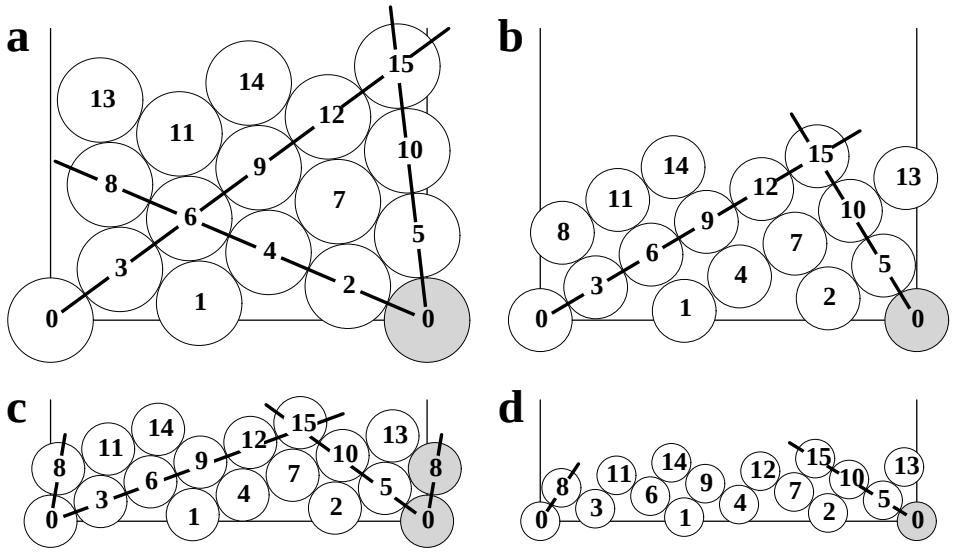

Figure 4.13: Patterns of tangent circles drawn on the surface of a cylinder as a function of circle diameter

The problem is to determine values of δ_m and δ_n. They are not simply functions of parameters m and n. Figure 4.13 shows that, for a given m and n, the values of δ_m and δ_n can be chosen from a certain range, yielding parastichies of different steepness. In order to determine this range, observe that at its limits the phyllotactic pattern changes; one previously evident parastichy disappears and another is formed. Thus, at the range limit, *three* evident parastichies coexist. It follows from Figure 4.13 that at one end of the range the third parastichy has order $|m-n|$, and at the other end it has order $(m+n)$. Three coexisting parastichies imply that each circle is tangent to six other circles. In other words, all circles lie in the vertices of a regular hexagonal grid, as seen in Figure 4.13a and c. Consequently, the angle $\beta + \gamma$ at vertex mn (Figure 4.12) is equal to $2\pi/3$. Expressing the base of the triangle in terms of its two sides and their included angle results in

$$(2\pi)^2 = (nd)^2 + (md)^2 - 2(nd)(md)\cos(2\pi/3)$$

or, after simplification,

$$d = 2\pi/\sqrt{m^2 + mn + n^2}. \tag{4.10}$$

Equations (4.9) and (4.10) yield

$$n\delta_m + m\delta_n = 2\pi(n^2 - m^2)/(m^2 + mn + n^2). \tag{4.11}$$

Solving the system of equations (4.5) and (4.11) with respect to δ_m and δ_n produces

$$\delta_m = \pi(m + 2n)/(m^2 + mn + n^2) \tag{4.12}$$

and

$$\delta_n = \pi(2m + n)/(m^2 + mn + n^2). \tag{4.13}$$

Given the values of δ_m and δ_n, the divergence angle α can be found from either equation (4.3) or (4.4), assuming that the encyclic numbers Δ_m or Δ_n are known. It follows from the definition that these numbers are the *smallest* positive integers satisfying equation (4.6). A systematic method for solving this equation, based on the theory of continuous fractions, is presented by van Iterson [75]. Erickson [36] points out that in practice the solution can often be found by guessing. Another possibility is to look for the smallest pair of numbers (Δ_m, Δ_n) satisfying (4.6) using a simple computer program.

Pattern construction

In conclusion, a phyllotactic pattern characterized by a pair of numbers (m, n) can be constructed as follows:

1. Find Δ_m and Δ_n from equation (4.6).
2. Find the range of admissible values of the angular displacements δ_m and δ_n. The limits can be obtained from equations (4.12) and (4.13) using the values of m and n for one limit, and the pair $(\min\{m, n\}, |m - n|)$ for the other.
3. For a chosen pair of admissible displacement values δ_m and δ_n, calculate the divergence angle α from equation (4.3) or (4.4) and the vertical displacement h from equation (4.8).
4. Find the diameter d of the circles from equation (4.8).

The diameter d does not enter directly in any formula used for image synthesis, but serves as an estimate of the size of surfaces to be incorporated in the model. This algorithm was applied to produce Table 4.1 showing parameter values for which three parastichies coexist. Given a pattern with two parastichies, this table provides the limits of the divergence angle α. For example, a (5,8) pattern can be formed for values of α ranging from 135.918365° to 138.139542°, which correspond to the patterns (3,5,8) and (5,8,13), respectively.

Triple-contact patterns

Further information relating the divergence angle α to the vertical displacement h for various phyllotactic patterns is shown in Figure 4.14. The arcs represent parameters of patterns with two parastichies (m, n). The branching points represent parameters of patterns with three parastichies $(m, n, m + n)$.

m,n,m+n	α (degrees)	h	d
(1, 1, 2)	180.000000	1.81380	-
(1, 2, 3)	128.571426	0.777343	2.374821
(1, 3, 4)	96.923073	0.418569	1.742642
(2, 3, 5)	142.105270	0.286389	1.441462
(1, 4, 5)	77.142860	0.259114	1.371104
(3, 4, 7)	102.162163	0.147065	1.032949
(3, 5, 8)	135.918365	0.111049	0.897598
(2, 5, 7)	152.307693	0.139523	1.006115
(1, 5, 6)	63.870968	0.175529	1.128493
(4, 5, 9)	79.672134	0.089203	0.804479
(4, 7, 11)	98.709671	0.058510	0.651536
(3, 7, 10)	107.088600	0.068878	0.706914
(3, 8, 11)	131.752579	0.056097	0.637961
(5, 8, 13)	138.139542	0.042181	0.553204
(5, 7, 12)	150.275223	0.049921	0.601820
(2, 7, 9)	158.507462	0.081215	0.767613

Table 4.1: Cylinder formula values for triple-contact patterns

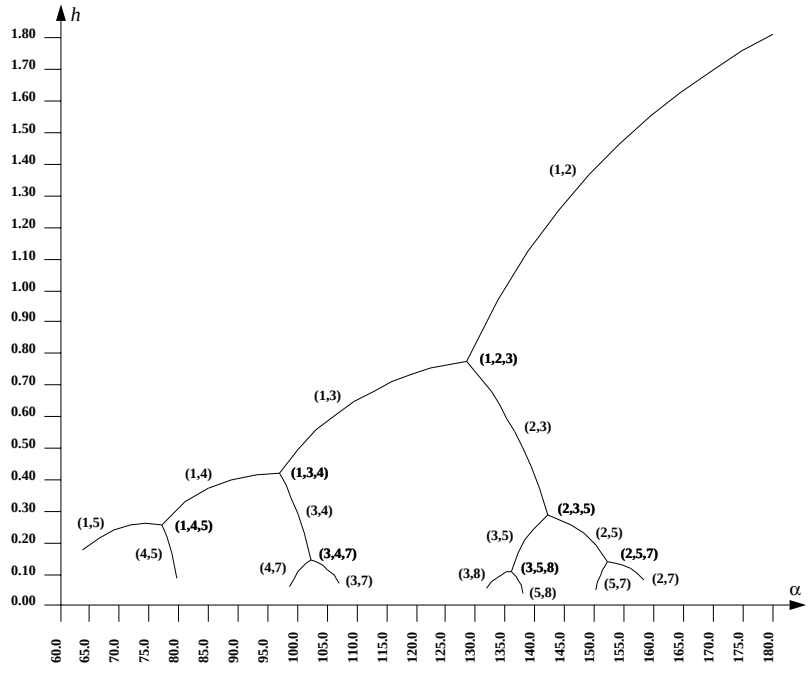

Figure 4.14: The vertical displacement h as a function of the divergence angle α for various phyllotactic patterns

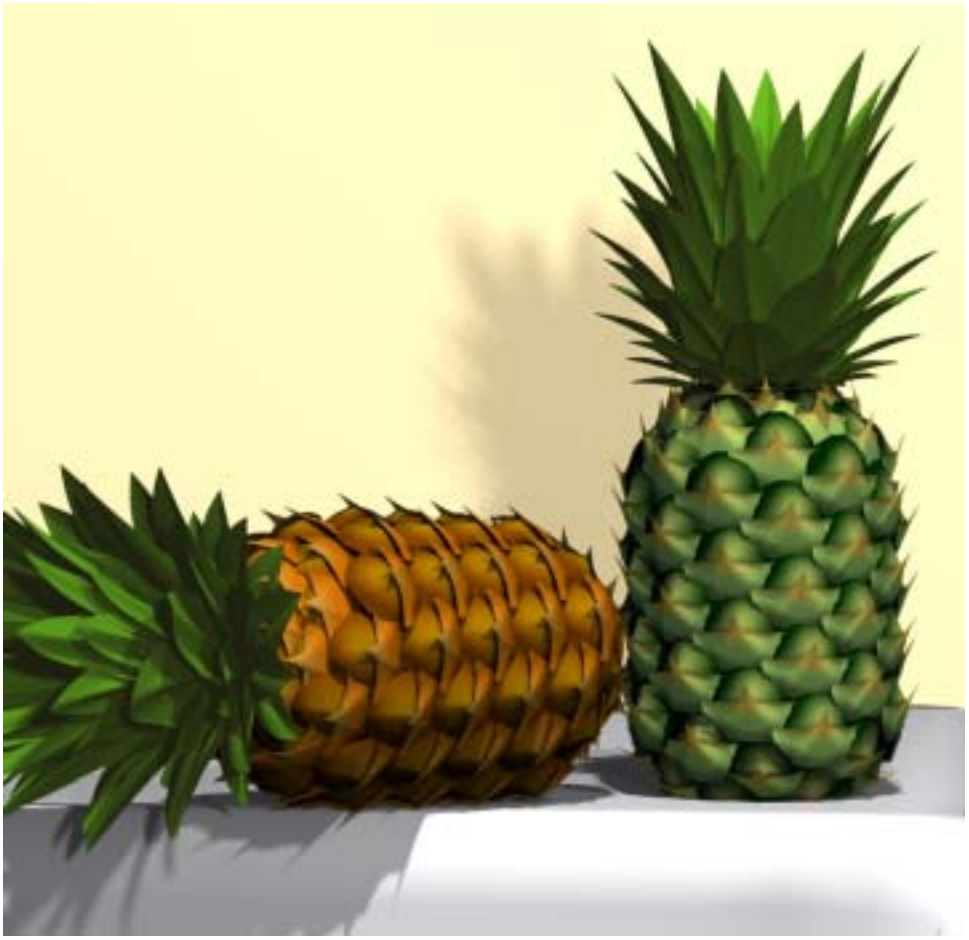

Figure 4.15: Pineapples

Pineapple

Spruce cones

Models of fruits synthesized using the cylindrical model are shown in Figures 4.15 and 4.16. The pineapple (Figure 4.15) is an example of a pattern where a given scale has six neighbors, which belong to 5-, 8- and 13-parastichies. The corresponding divergence angle α is equal to 138.139542°. The spruce cones (Figure 4.16) were generated using the values $m = 5$, $n = 8$ and $\alpha = 137.5°$ (the divergence angle α for a $(5, 8)$-parastichy pattern belongs to the interval 135.918365° to 138.139542°). From these values, h and d were calculated as a function of the radius of the cylinder. The effect of closing the bottom and top of the pineapple and spruce cones was achieved by decreasing the diameter of the cylinder and the size of the scales.

Sedge

A variant of the model of phyllotaxis on a cylinder can be used to model organs that are conical rather than cylindrical in shape. For example, Figure 4.17 shows a model of the sedge *Carex laevigata*. L-system 4.1 generates the male spike. Production p_1 specifies the basic

Figure 4.16: Spruce cones

Figure 4.17: *Carex laevigata*: the male spike, the entire shoot, the female spike

```
#define IRATE 1.025 /* internode growth rate */
#define SRATE 1.02  /* spikelet growth rate */
#include M           /* spikelet shape specification */

ω  :  A
p1 :  A    :  *    → [&(5)f(1)~M(1)]F(0.2)/(137.5)A
p2 :  M(s) :  s<3  → M(s*SRATE)
p3 :  f(s) :  s<3  → f(s*SRATE)
p4 :  &(s) :  s<15 → &(s*SRATE)
p5 :  F(i) :  i<1  → F(i*IRATE)
```

L-system 4.1: The male spike of *Carex laevigata*

layout of the spikelets, similar to that given by the L-system in Figure 4.11. The top portion of the spike has a conical shape due to the growth of spikelets for some time after their creation by the apex. According to production p_2, a spikelet grows by factor $SRATE$ in each derivation step, until it reaches the threshold size of 3. In an analogous way, productions p_3, p_4 and p_5 capture the distance increase between spikelets and the spike axis, the increase of the branching angle, and the elongation of internodes.

The models of phyllotaxis deal with the arrangement of organs in space. For the purpose of mathematical analysis their shape is reduced to a simple geometric figure, usually a circle. However, in realistic images the exact shape of the organs must be captured as well. Several techniques suitable for this purpose are outlined in the next chapter.